NANO LETTERS

2007
Vol. 7, No. 1
15−21

Nanoscopically Flat Open-Ended Single-Walled Carbon Nanotube Substrates for Continued Growth

Myung Jong Kim,[†,‡] Erik Haroz,[‡] Yuhuang Wang,[‡,§] Hongwei Shan,[‡] Nolan Nicholas,[†,‡] Carter Kittrell,[*,‡,§] Valerie C. Moore,[‡,§] Yeonwoong Jung,[||] David Luzzi,[||] Robert Wheeler,[⊥] Tia BensonTolle,[⊥] Hua Fan,[†,‡] Sean Da,[#] Wen-Fang Hwang,[‡] T. J. Wainerdi,[‡] Howard Schmidt,[‡] Robert H. Hauge,[*,‡,§] and Richard E. Smalley[†,‡,§]

Department of Physics & Astronomy, Department of Chemistry, and Carbon Nanotechnology Laboratory, Rice University, 6100 Main Street, MS-100, Houston, Texas 77005, Department of Materials Science & Engineering, University of Pennsylvania, 3231 Walnut Street, Philadelphia, Pennsylvania 19104-6272, Structural Materials Branch, 2941 Hobson Way, Wright-Patterson Air Force Base, Ohio 45433-7750, and FEI Company, 5350 NE Dawson Creek Drive, Hillsboro, Oregon 97124

Received July 3, 2006; Revised Manuscript Received October 12, 2006

ABSTRACT

Continued growth is a way of growing nanotubes targeted to produce continuous and chirality-controlled single-walled carbon nanotube (SWNT) materials. This growth method strongly depends on efficient preparation of open-ended SWNT substrates. Nanoscopically flat open-ended SWNT substrates have been prepared by cutting the SWNT spun fiber with a focused ion beam cutting technique and followed by etching schemes for cleaning amorphous carbon and opening the ends of the SWNTs. The open ends were effectively characterized through selective etch back of open SWNT ends by carbon dioxide gas at 950 °C. High density continued growth was demonstrated from these nanoscopically flat open-ended substrates.

Single-walled carbon nanotubes (SWNTs) are currently the focus of intensive interdisciplinary study due to their remarkable physical and chemical properties and their prospects for various scientific and practical applications ranging from electronic to biological devices.[1] For electronic application, chirality selected SWNTs are critical in both macroscopic (armchair quantum wire[2]) and microscopic applications (field effect transistors[3]). So far, no growth method including arc discharge,[4,5] laser ablation,[6] and chemical vapor deposition[7−11] has been able to control the chirality of SWNTs. The ability to reinitiate growth from a pre-existing open-ended SWNT seed combined with a separation technique[12−14] is uniquely desirable to produce a large quantity of chirality selected SWNT materials.

Continued growth of SWNTs[15] is a way of growing nanotubes targeted to produce continuous and chirality-controlled SWNT materials. Starting from a periodic array of open-ended SWNTs, so-called "open-ended SWNT substrates", nanometer-sized catalyst particles are docked to the open ends and act to decompose introduced carbon feedstock adding carbon atoms to a pre-existing carbon lattice. On the scale of an individual nanotube, this process is one-dimensional epitaxy with assistance of a catalyst following a tip growth mechanism by lifting off catalyst such that the growth would not be terminated by diffusion of carbon feedstock as base growth would.[16] If armchair open-ended substrates are prepared, this will provide an efficient mechanism to produce macroscopic armchair wires.

Continued growth of SWNTs highly depends on efficient preparation of open-ended SWNT substrate. Previously, our group demonstrated continued growth of SWNTs from an open-ended SWNT substrate prepared by a microtome

* Corresponding authors: Dr. Robert H. Hauge, tel 713-348-6384, fax 713-348-5320, e-mail hauge@rice.edu; Mr. Carter Kittrell, tel 713-348-5108, fax 713-348-5320, e-mail kittrell@rice.edu.
† Department of Physics & Astronomy, Rice University.
‡ Carbon Nanotechnology Laboratory, Rice University.
§ Department of Chemistry, Rice University.
|| Department of Materials Science & Engineering, University of Pennsylvania.
⊥ Structural Materials Branch, Wright-Patterson AFB.
FEI Company.

10.1021/nl061531+ CCC: $37.00
Published on Web 12/14/2006

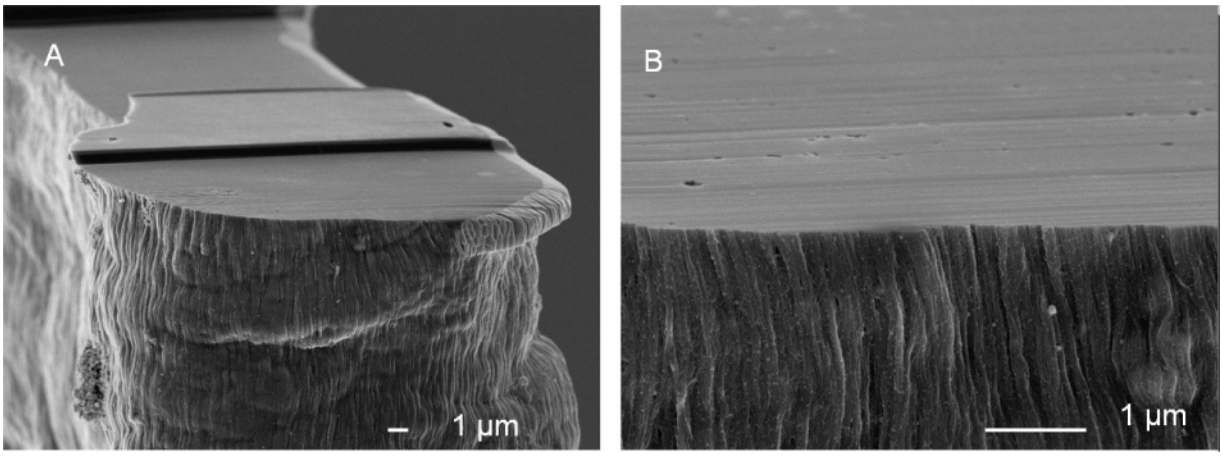

Figure 1. (A) The SEM image showing side view of FIB cut surface. (B) High magnification SEM image taken from the edge shows that the top surface is smoothly covered by amorphous carbon caused by ion damage or carbon redeposition.

cutting technique.[15] However, microtoming of the SWNT spun fiber[17] generated a "combed layer" where sidewalls of nanotubes are exposed. Etching of this layer requires a long exposure of oxygen plasma, which forms rough surfaces with 300−500 nm features (Figure 2C). Due to insufficient mutual support, tubes grown by this method from a microtomed substrate fell over. This is thought to be due either to the roughened surface morphology or to a decrease in the density of open-ended tubes due to long (∼20 min) oxygen plasma exposure.

To prepare nanoscopically flat open-ended substrates, focused ion beam cutting and polishing was employed. In focused ion beam cutting, an ion beam is scanned in a line on a surface producing a trench with an inverse Gaussian shape as expected from the beam profile. However, when the dose is increased, the trench becomes very sharp, narrow, and unexpectedly deep.[18] Previously, our group reported a preparation of a "bed-of-nails" membrane of SWNTs using a focused ion beam (FIB),[19] but an amorphous carbon cleaning and end opening schemes for open-ended SWNT substrates are reported here for the first time. Also, demonstrated continued growth with a high density is crucial evidence that efficient open-ended substrates were prepared. All the methods herein reported to prepare nanoscopically flat open-ended SWNT substrate are useful not only for continued growth of SWNTs[15] but also for open-ended nanotube-based membrane filters[20,21] or studies of the chemical and physical properties of SWNT ends.[22]

FIB cutting on the SWNT spun fiber was performed by our collaborators in AFB, UPenn, and FEI using a FEI Strata DB235 focused ion beam. A gallium ion (Ga^+) beam was used as an ion source and focused down to a 10−20 nm sized spot. Accelerated gallium ions transfer a great deal of momentum, sputtering carbon atoms from the lattice so that true cutting of tubes is achieved. The procedure is comprised of two parts, cutting and polishing. An acceleration voltage of 10 kV and current of 500−1000 pA were used for rough cutting, and voltage and current of 10 kV and 100−500 pA were used for polishing. The polishing cycle was repeated until most of artifacts generated by cutting were removed. Finally, a nanoscopically flat surface was revealed after two processes (Figure 1).

The surface is very smooth, but it is covered by amorphous carbon and implanted gallium. The amorphous carbon layer is produced by ion damage resulting from the displacement of atoms from their lattice sites due to collisions with the ions or by redeposition of carbon atoms caused by a back scattering process. Furthermore, the ends of the tubes might be closed by the heat generated or by carbon redeposition. Thus, we need a cleaning process to remove Ga and amorphous carbon and an end opening step.

After FIB cutting, the 7−10 mm long fiber pieces were dipped into a 1:1 MeOH/1 N HCl solution at 60 °C overnight (about 8 h). Methanol was added for better wetting ability that enables the HCl to penetrate into the surface of the fiber by capillary action. Since the melting temperature of Ga is so low (T_m = 29.77 °C), at 60 °C, it should be in a liquid state that will easily react with HCl. To avoid evaporation of the solution from the beaker, a watch glass was laid on top of the beaker, so that vapor was condensed back into the solution. Through this step, most of the embedded Ga has been removed as shown by EDX (energy dispersive X-ray analysis) data (Supporting Information **S1**).

To minimize the effects of residual catalyst particles in the fiber, H_2 baking at elevated temperature followed by dipping the fiber into 1 N HCl solution was performed. In each cycle, temperature was ramped in three steps (110, 350, 800 °C) while resting at each step for 1 h in 10% H_2 balanced with Ar at 1 atm total pressure. After the first H_2 baking, the catalyst particles were exposed at the surface of the fiber, mobilized by heat and hydrogen in a manner similar to Ostwald ripening and then were subsequently removed by HCl (Figure 2A,B). This cycle was repeated until no catalyst was observed at the surface after hydrogen baking. Usually, two or three cycles were enough, but this process could not remove the amorphous carbon layer.

Two techniques have been successfully developed for removing amorphous carbon. The first one is hydrogen cleaning with assistance of catalysts in a HV reactor with a laser heating system similar to what has been described in

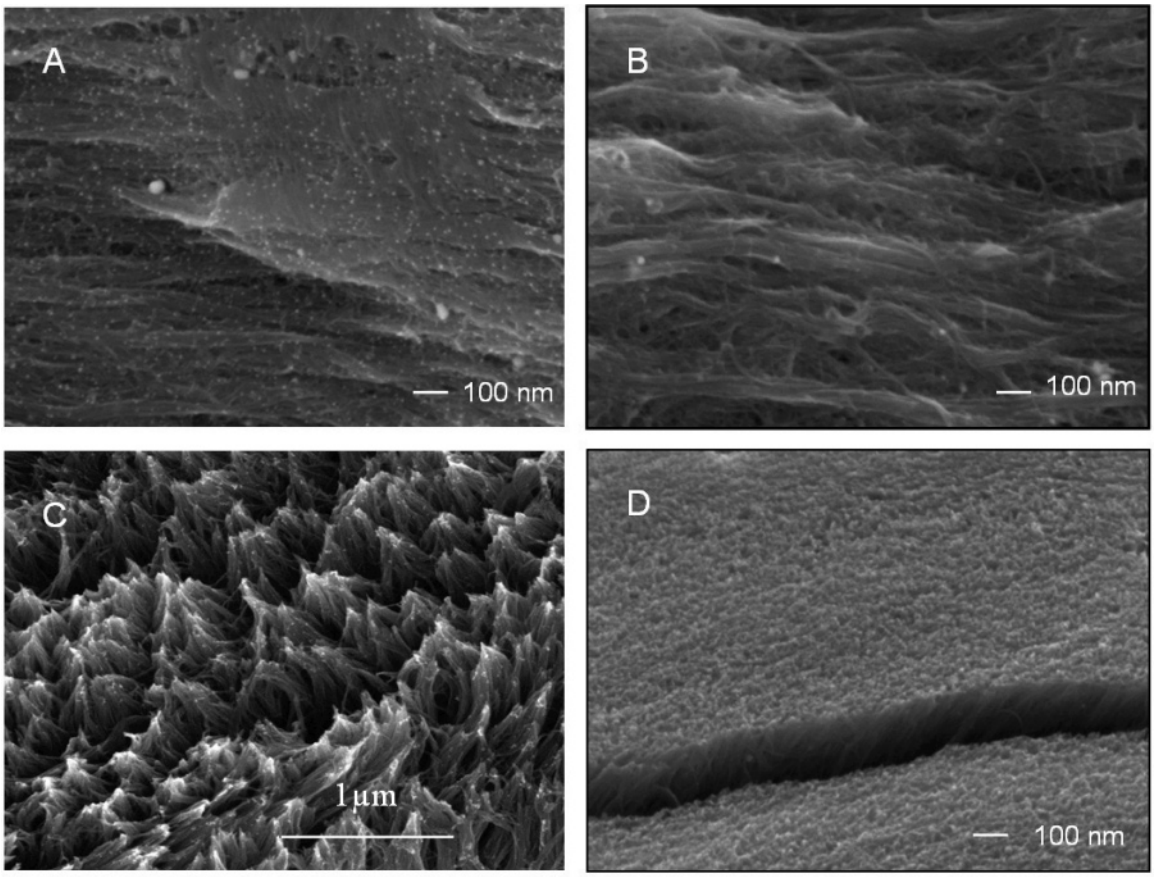

Figure 2. (A, B) Residual catalysts cleaning. (A) SEM image taken after hydrogen baking at the side of the fiber. (B) The SEM image shows that catalyst particles at the surface were cleaned by dipping the fiber into 1 N HCl. (C, D) Comparison of open-ended substrates. (C) An open-ended substrate prepared by microtome cutting and followed by etching and cleaning steps shows a rough surface with 300−500 nm features. (D) An open-ended substrate prepared by FIB cutting and followed by cleaning step shows nanoscopically flat surface. (The sample was cleaned with 1 Torr H_2 at 750 °C in a HV chamber with assistance of Fe/Ni catalyst, and the SEM image was taken at the naturally formed crack showing dense and clean SWNT bundles.)

the previous article.[15] A very thin layer (2.8 Å) of Fe/Ni catalyst was evaporated onto the cross sectional surface of the fiber at about 350 °C in a reducing environment of 1×10^{-5} Torr of hydrogen. Subsequently, hydrogen was introduced and maintained at 1 Torr pressure at 750 °C for 40 min. After hydrogen cleaning, the fiber was dipped into 1 N HCl solution to remove catalyst. Finally, a nanoscopically flat (∼10 nm surface roughness) and very clean SWNT substrate was revealed as shown in Figure 2D.

Carbon dioxide has been found to be very effective for removing amorphous carbon without requiring any catalyst. It is known that CO_2 itself cannot etch graphite below 900 °C in the absence of catalyst.[23] As illustrated in panels A and C of Figure 4, it has been found that the amorphous layer on the surface was completely removed by 10% CO_2 balanced with argon at 950 °C for 20 min in a quartz tube furnace without causing any damage to the nanotubes at the surface. We then tried an additional 20 min, but the surface remained the same and also flat. Thus, we suspected that the ends of tubes might be closed because the edge of the graphite will begin to etch around 900 °C.[23]

For preparing an open-ended SWNT substrate, a characterizing method for open ends is crucial because it is not possible to grow tubes continuously from closed-ended tubes. Previous studies for characterizing open-ended tubes were limited to gas adsorption techniques,[24,25] which are not feasible for less than a 100 μm diameter surface of the fiber. Transmission electron microscopy might be another means, but it does not have the capability of giving information of the overall surface. Taking advantage of the observation that 10% of CO_2 could not etch back the tubes at the surface at 950 °C, we proceeded to try the same condition to a HOPG (highly ordered pyrolytic graphite) surface and open-ended SWNTs. The step edges on HOPG surface were etched back with a 2−3 nm/min etching rate by 10% of CO_2 at 950 °C for 15 min. Also, open-ended SWNT bundles (the purified tubes[26] are considered as open-ended tubes because catalyst particles were detached off during the purification process.) were etched back by a series of 120 pulses of CO_2 at 950 °C. The pulsed etching scheme was adopted to not remove all the short bundles. Each pulse contains 55 mL of CO_2 yielding 300 ms, 1 atm exposure to the sample separated by 1 min of Ar at 1 atm. This experiment leads us to believe that CO_2 gas can etch back only open-ended tubes at 950 °C; this became a powerful tool for testing an end-opening scheme (Figure 3).

To open the ends of SWNTs, various methods have been tried including wet chemical methods such as hot

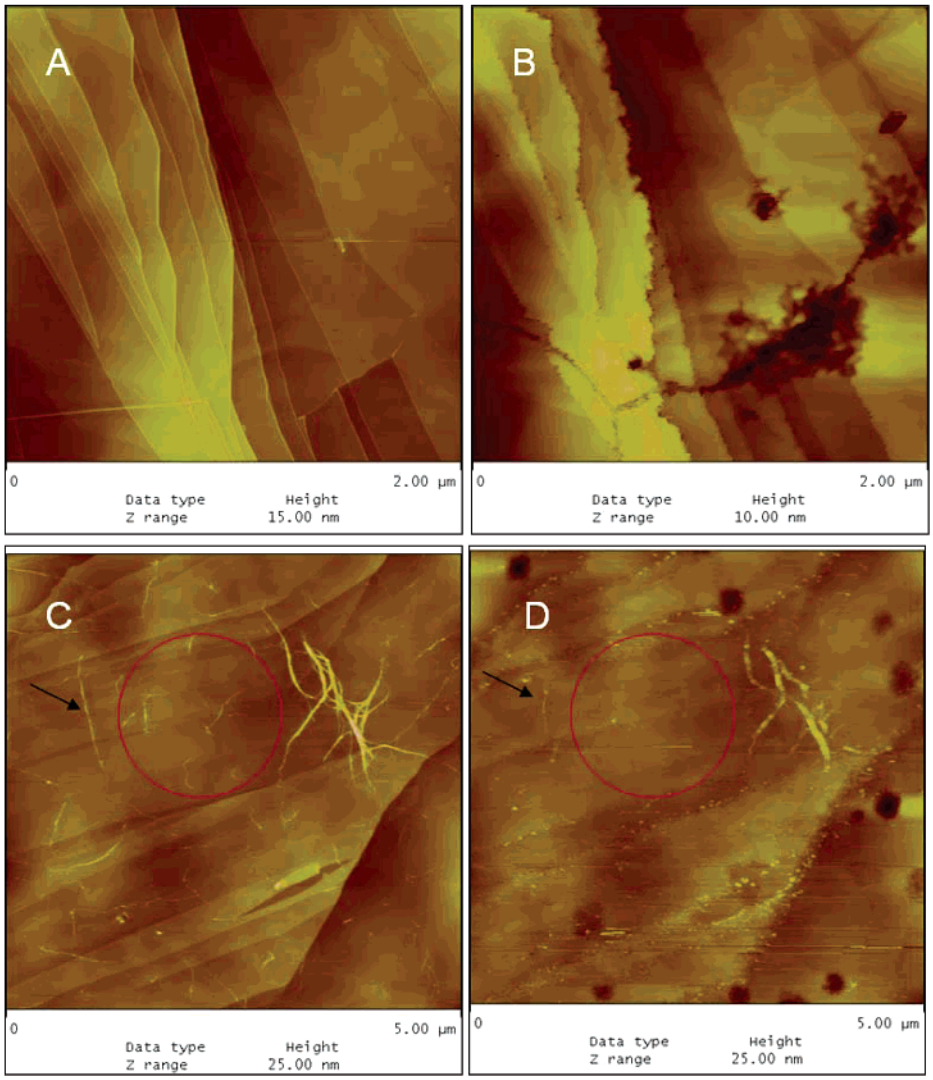

Figure 3. AFM images of CO_2 etching for open end characterization. (A, B) Before and after images of CO_2 etching on HOPG surface show that the step edges of graphite can be etched by 10% CO_2 at 950 °C. (C, D) Before and after images of CO_2 etching on open-ended SWNT bundles show that the open-ended tubes can be etched by 10% CO_2 at 950 °C. (Purified tubes were used for this experiment, and those are considered as open-ended tubes because catalyst was detached off during the purification step.)

and cold piranha[27](4:1, vol/vol 96% H_2SO_4/30% H_2O_2), $KMnO_4$,[28] and electrochemistry,[29] but most of the wet chemical methods turned out to have a problem of producing a surface oxide layer. Two clean methods of opening the ends of tubes were found to be a very short exposure of inductively coupled oxygen plasma and Ar ion sputtering, respectively. The prepared flat and clean SWNT substrate was exposed to inductively coupled oxygen plasma for 10−20 s. Panels A and B of Figure 4 showed that there was almost no change after 20 s of exposure to inductively coupled oxygen plasma, and no surface oxide was found to be formed on the surface. After the sample was treated with 10% of CO_2 at 950 °C in a quartz tube furnace, the morphology has been significantly changed, and the surface roughness had increased from about 10 nm to about 200 nm as illustrated in panels C and D of Figure 4. This leads us to believe that short exposure to inductively coupled plasma is an effective means to open the ends of the tubes in our substrate.

As an alternative method, Ar ion sputtering was also developed. Ar ion impact can generate vacancies by knock-on or cascade processes without any contamination. The 3CM DC (CSC, Veeco) ion source was employed, and the experiment was performed at current density 0.25 mA/cm^2 and 500 V acceleration voltage at a normal angle to the surface for 1 min (15 mC/cm^2 total charge). Ar ion sputtering by itself did not cause any morphology change, but sputtering followed by 10% CO_2 etching at 950 °C for 20 min in a quartz tube furnace increased surface roughness (Supporting Information **S2**). This indicates that Ar ion sputtering is also a means of opening the ends of the tubes or introducing other defects exploitable by CO_2 etching.

After the ends of the tubes were opened, a very thin layer (2.1 Å) of Fe/Ni catalyst was deposited from the e-beam evaporator in a reducing environment of 1×10^{-5} Torr of hydrogen at about 350 °C. Since the surface is nanoscopically flat and highly dense, most of deposited catalyst atoms are expected to dock to the open ends of the tubes directly,

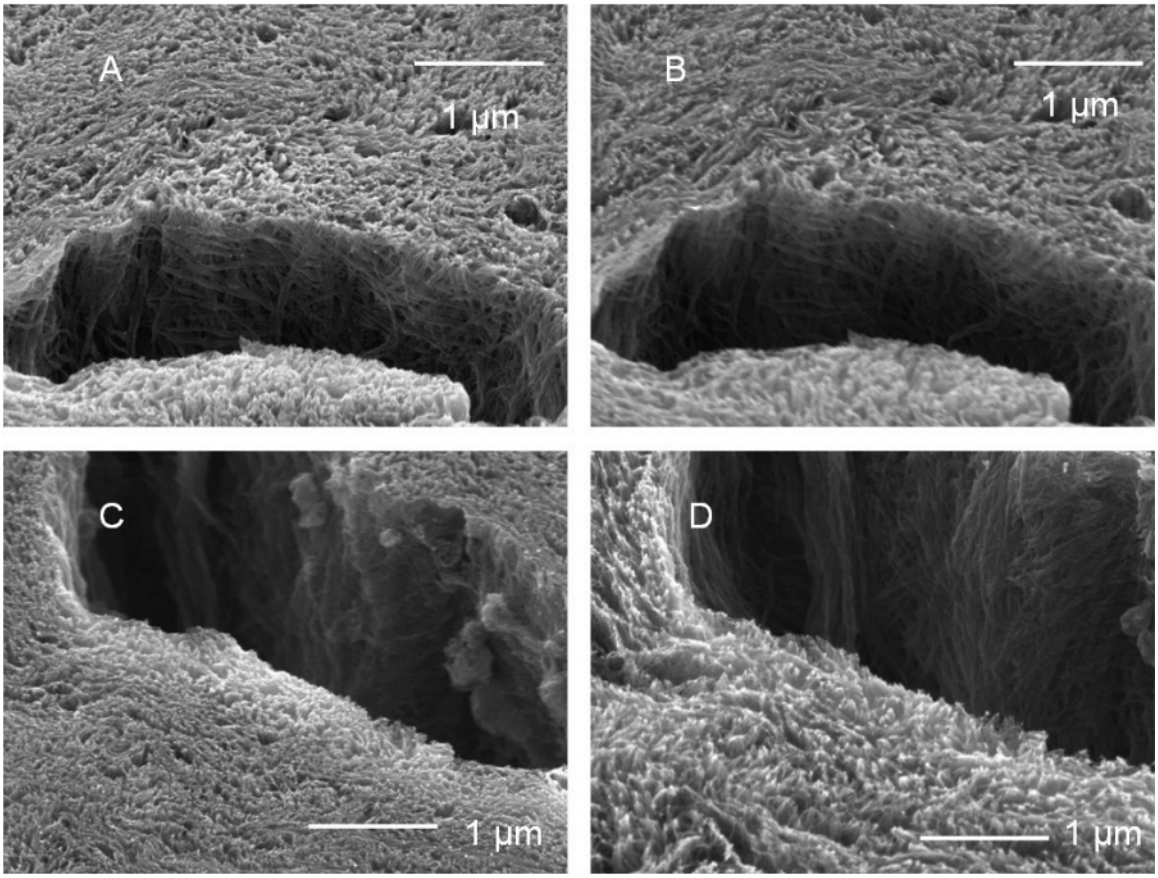

Figure 4. End opening scheme with short exposure to oxygen plasma. (A) The SEM shows that amorphous carbon was cleaned with 10% CO_2 at 950 °C for 20 min in a quartz tube furnace. (B) SEM images taken after treatment with inductively coupled oxygen plasma for 20 s shows no visible change. (C) SEM image taken after cleaning amorphous carbon with 10% CO_2 at 950 °C for 20 min in a quartz tube furnace. (D) SEM image taken after the oxygen plasma treatment followed by 10% of CO_2 etching at 950 °C for 20 min shows significant morphology change indicating that closed ends can be etched open by short exposure to inductively coupled oxygen plasma.

otherwise they will slightly diffuse around the side of the tubes and find the ends of the tubes because the ends are more reactive compared to the sidewall of the tube. Through this process, more uniform diameter sized particles are expected to be nucleated and grow on the open ends.

As soon as the catalyst was deposited, ethanol was introduced without hydrogen and maintained at 10 Torr by an automated throttle valve and feedback control. The temperature was increased to 800 °C within 2 min to avoid non-nanotube carbon deposition such as amorphous carbon that might cause catalyst poisoning. The growth time was 30 min, and the 2−3 μm extension of the fiber was observed in the real time image from a CCD camera. As illustrated in panels A and B of Figure 5, a significant change has been observed after the growth experiment. Bundles of tubes have grown up seamlessly from the SWNT substrate. The scanning electron microscopy (SEM) image (panel C of Figure 5) taken from the edge of the fiber shows that the grown tubes are aligned vertically. This indicates that the tubes were grown with high density, and vertical growth was not observed from the sample prepared by microtome cutting and an oxidative etching scheme.

The Raman data (**S4** in Supporting Information) support the belief that the grown tubes are not tubes of new chirality but tubes of the same chirality as the SWNT substrate, showing that the RBM peaks taken before and after growth experiment peaks all match in terms of their wave numbers (peak position) because the peak position of the RBM peaks represents chirality of SWNTs in Raman spectra.[30] Raman data were collected with a Raman microscope (Renishaw Micro-Raman System 1000) using the three laser excitation lines (514, 633, 780 nm) to excite many chiralities of nanotubes because Raman data we collect is caused by resonant Raman scattering that occurs when the energy of the laser matches the interband transition energy of the nanotube.[30] To collect Raman signal from the top surface, the 2 μm diameter spot (50× objective) of the laser was focused onto the top surface, and the sample was tilted at a 45° angle from the direction of the laser so that we could avoid polarization mismatch.[31] We collected spectra from several spots, and they agree with each other in terms of the wave number of the RBM.

In conclusion, nanoscopically flat open-ended substrates were prepared by cutting the spun fiber perpendicular to the fiber axis with FIB and followed by cleaning and end-opening steps. The open ends were characterized by CO_2 gas at 950 °C showing selective etch-back. Continued growth was demonstrated from these substrates. The fact that grown tubes were vertically aligned indicates that high-density growth has been achieved from efficiently prepared open-

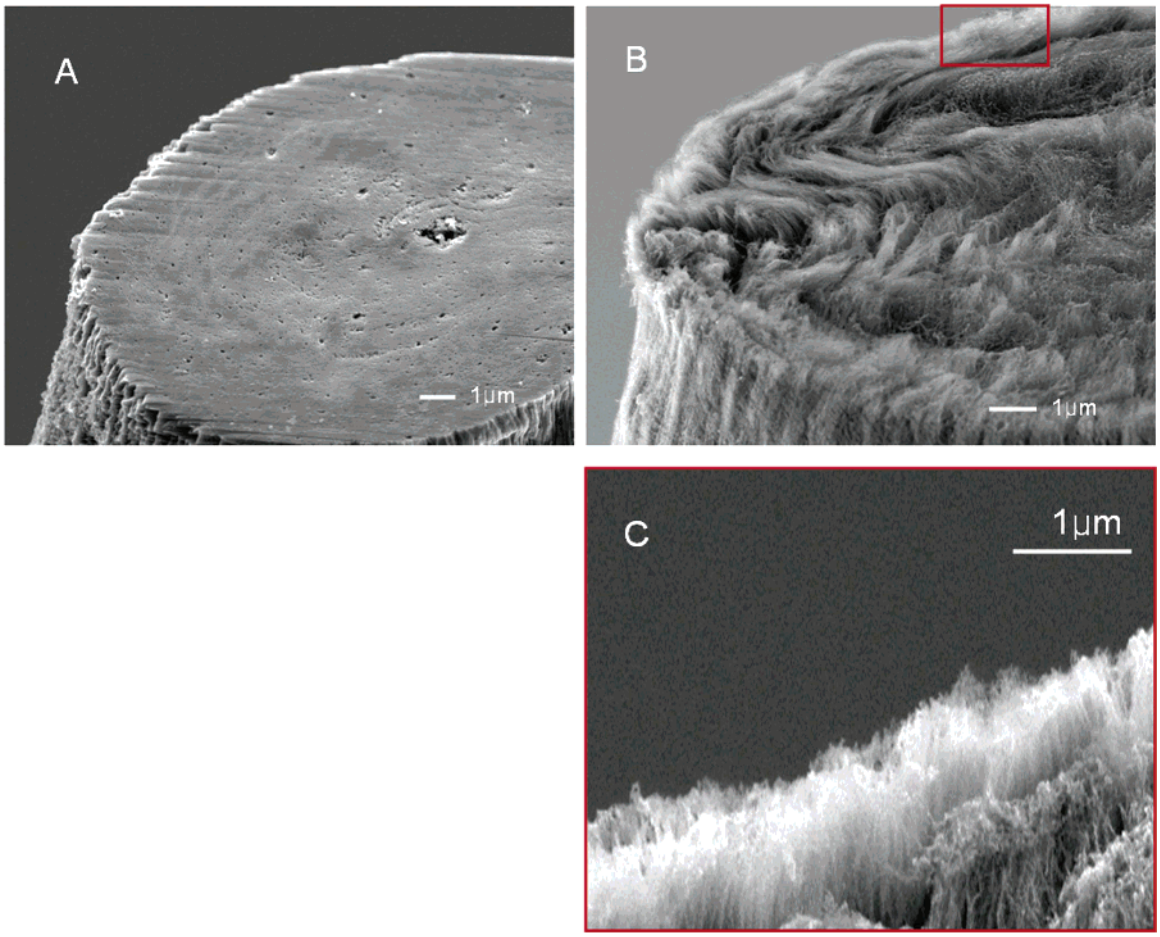

Figure 5. (A) SEM image taken from nanoscopically flat SWNT substrate after FIB cutting. (B) SEM image taken after the growth experiment. (C) High magnification images taken from the edge (red square) of the fiber after growth experiment. This image shows that the density of nanotubes is high enough to be grown vertically.

ended substrates by a FIB cutting technique and followed by amorphous carbon cleaning and end-opening schemes. From a comparison of the RBMs obtained from the before and after spectra out of the fiber, it appears highly suggestive that the new growth is indeed from the continued growth of pre-existing SWNTs and not nucleation of new tubes.

Acknowledgment. We gratefully acknowledge Steve Ripley for technical support, Dr. Sivaram Arepalli for helpful discussion, Professor Douglas Natelson and Sungbae Lee for Ar ion sputtering, Dr. Bruce R. Johnson for managing the REU program that provided summer students. This work was supported by Department of Energy (DE-AC05-00OR22725) through the Oakridge National Laboratory, NASA (NCC 9-77), and the Robert A. Welch Foundation (C-0689). Myung Jong Kim gratefully acknowledges the Dr. Zabel memorial fund award.

Supporting Information Available: **(S1)** EDX (energy dispersive X-ray analysis) data of FIB cut surface, **(S2)** end opening scheme with sputtering (SEM data), **(S3)** continued growth reactor (schematic drawing and a picture), **(S4)** Raman data taken before and after growth experiment, and **(S5)** controlled experiment with closed-ended substrates. This material is available free of charge via the Internet at http://pubs.acs.org.

References

(1) Dresselhaus, M. S.; Dresselhaus, G.; Avouris, P. *Carbon Nanotubes Synthesis, Structure, Properties and Applications*; Springer: Berlin, 2001.
(2) Smalley, R. E. *Review of Non-Oil and Gas Research Activities in the Houston-Galveston-Gulf Coast Area*; Rice University: Houston, 12/4/2003, 2003; pp 1−4.
(3) Tans, S. J.; Verschueren, A. R. M.; Dekker, C. Room-Temperature Transistor Based On a Single Carbon Nanotube. *Nature* **1998**, *393* (6680), 49−52.
(4) Iijima, S.; Ichihashi, T. Single-Shell Carbon Nanotubes of 1-nm Diameter. *Nature* **1993**, *363* (6430), 603−615.
(5) Bethune, D. S.; Kiang, C. H.; Devries, M. S.; Gorman, G.; Savoy, R.; Vazquez, J.; Beyers, R. Cobalt-Catalyzed Growth of Carbon Nanotubes with Single-Atomic-Layerwalls. *Nature* **1993**, *363* (6430), 605−607.
(6) Thess, A.; Lee, R.; Nikolaev, P.; Dai, H. J.; Petit, P.; Robert, J.; Xu, C. H.; Lee, Y. H.; Kim, S. G.; Rinzler, A. G.; Colbert, D. T.; Scuseria, G. E.; Tomanek, D.; Fischer, J. E.; Smalley, R. E. Crystalline Ropes of Metallic Carbon Nanotubes. *Science* **1996**, *273* (5274), 483−487.
(7) Li, Y. M.; Kim, W.; Zhang, Y. G.; Rolandi, M.; Wang, D. W.; Dai, H. J. Growth of single-walled carbon nanotubes from discrete catalytic nanoparticles of various sizes. *J. Phys. Chem. B* **2001**, *105* (46), 11424−11431.
(8) An, J. W.; Lim, D. S. Synthesis and characterization of alumina/carbon nanotube composite powders. *J. Ceram. Process. Res.* **2002**, *3* (3), 174−177.

(9) Murakami, Y.; Chiashi, S.; Miyauchi, Y.; Hu, M. H.; Ogura, M.; Okubo, T.; Maruyama, S. Growth of vertically aligned single-walled carbon nanotube films on quartz substrates and their optical anisotropy. *Chem. Phys. Lett.* **2004**, *385* (3−4), 298−303.
(10) Eres, G.; Kinkhabwala, A. A.; Cui, H. T.; Geohegan, D. B.; Puretzky, A. A.; Lowndes, D. H. Molecular beam-controlled nucleation and growth of vertically aligned single-wall carbon nanotube arrays. *J. Phys. Chem. B* **2005**, *109* (35), 16684−16694.
(11) Hata, K.; Futaba, D. N.; Mizuno, K.; Namai, T.; Yumura, M.; Iijima, S. Water-assisted highly efficient synthesis of impurity-free single-walled carbon nanotubes. *Science* **2004**, *306* (5700), 1362−1364.
(12) Krupke, R.; Hennrich, F.; von Lohneysen, H.; Kappes, M. M. Separation of metallic from semiconducting single-walled carbon nanotubes. *Science* **2003**, *301* (5631), 344−347.
(13) Krupke, R.; Hennrich, F.; Kappes, M. M.; Lohneysen, H. V. Surface conductance induced dielectrophoresis of semiconducting single-walled carbon nanotubes. *Nano Lett.* **2004**, *4* (8), 1395−1399.
(14) Strano, M. S.; Dyke, C. A.; Usrey, M. L.; Barone, P. W.; Allen, M. J.; Shan, H. W.; Kittrell, C.; Hauge, R. H.; Tour, J. M.; Smalley, R. E. Electronic structure control of single-walled carbon nanotube functionalization. *Science* **2003**, *301* (5639), 1519−1522.
(15) Wang, Y. H.; Kim, M. J.; Shan, H. W.; Kittrell, C.; Fan, H.; Ericson, L. M.; Hwang, W. F.; Arepalli, S.; Hauge, R. H.; Smalley, R. E. Continued growth of single-walled carbon nanotubes. *Nano Lett.* **2005**, *5* (6), 997−1002.
(16) Huang, S. M.; Woodson, M.; Smalley, R.; Liu, J. Growth mechanism of oriented long single walled carbon nanotubes using "fast-heating" chemical vapor deposition process. *Nano Lett.* **2004**, *4* (6), 1025−1028.
(17) Ericson, L. M.; Fan, H.; Peng, H. Q.; Davis, V. A.; Zhou, W.; Sulpizio, J.; Wang, Y. H.; Booker, R.; Vavro, J.; Guthy, C.; Parra-Vasquez, A. N. G.; Kim, M. J.; Ramesh, S.; Saini, R. K.; Kittrell, C.; Lavin, G.; Schmidt, H.; Adams, W. W.; Billups, W. E.; Pasquali, M.; Hwang, W. F.; Hauge, R. H.; Fischer, J. E.; Smalley, R. E. Macroscopic, neat, single-walled carbon nanotube fibers. *Science* **2004**, *305* (5689), 1447−1450.
(18) Meingailis, J. Focused ion beam technology. *J. Vac. Sci. Technol., B: Microelectron., Process. Phenom.* **1987**, *5* (2), 469−495.
(19) Wang, Y. H.; Da, S.; Kim, M. J.; Kelly, K. F.; Guo, W. H.; Kittrell, C.; Hauge, R. H.; Smalley, R. E. Ultrathin "bed-of-nails" membranes of single-wall carbon nanotubes. *J. Am. Chem. Soc.* **2004**, *126* (31), 9502−9503.
(20) Holt, J. K.; Park, H. G.; Wang, Y.; Stardermann, M.; Artyukhin, A. B.; Grigoropoulos, C. P.; Noy, A.; Bakajin, O. Fast Mass Transport Through Sub-2-Nanometer Carbon Nanotubes. *Science* **2006**, *312*, 1034−1037.
(21) Srivastava, A.; Srivastava, O. N.; Talapatra, S.; Vajtai, R.; Ajayan, P. M. Carbon, nanotube filters. *Nat. Mater.* **2004**, *3*, 610−613.
(22) Dean, K. A.; Chalamala, B. R. Experimental studies of the cap structure of single-walled carbon nanotubes. *J. Vac. Sci. Technol., B: Microelectron. Nanometer Struct.—Process., Meas., Phenom.* **2003**, *21* (2), 868−871.
(23) Walker, P. L.; Thrower, P. A. *Chemistry and Physics of Carbon*; Marcel Dekker: New York, 1981; Vol. 16, pp 54−61.
(24) Kleinhammes, A.; Mao, S. H.; Yang, X. J.; Tang, X. P.; Shimoda, H.; Lu, J. P.; Zhou, O.; Wu, Y. Gas adsorption in single-walled carbon nanotubes studied by NMR. *Phys. Rev. B* **2003**, *68* (7), 075418.
(25) Babba, M. R.; Stepanek, I.; Masenelli-Valot, K.; Dupont-Pavlovsky, N.; McRae, E.; Bernier, P. Opening of single-walled carbon nanotubes: evidence given by krypton and xenon adsorption. *Surf. Sci.* **2003**, *531*, 86−92.
(26) Xu, Y. Q.; Peng, H. Q.; Hauge, R. H.; Smalley, R. E. Controlled multistep purification of single-walled carbon nanotubes. *Nano Lett.* **2005**, *5* (1), 163−168.
(27) Ziegler, K. J.; Gu, Z. N.; Peng, H. Q.; Flor, E. L.; Hauge, R. H.; Smalley, R. E. Controlled oxidative cutting of single-walled carbon nanotubes. *J. Am. Chem. Soc.* **2005**, *127* (5), 1541−1547.
(28) Zhang, J.; Zou, H. L.; Qing, Q.; Yang, Y. L.; Li, Q. W.; Liu, Z. F.; Guo, X. Y.; Du, Z. L. Effect of chemical oxidation on the structure of single-walled carbon nanotubes. *J. Phys. Chem. B* **2003**, *107* (16), 3712−3718.
(29) Fang, H. T.; Liu, C. G.; Chang, L.; Feng, L.; Min, L.; Cheng, H. M. Purification of single-wall carbon nanotubes by electrochemical oxidation. *Chem. Mater.* **2004**, *16* (26), 5744−5750.
(30) Dresselhaus, M. S.; Dresselhaus, G.; Jorio, A.; Souza, A. G.; Saito, R. Raman spectroscopy on isolated single wall carbon nanotubes. *Carbon* **2002**, *40* (12), 2043−2061.
(31) Duesberg, G. S.; Loa, I.; Burghard, M.; Syassen, K.; Roth, S. Polarized Raman spectroscopy on isolated single-wall carbon nanotubes. *Phys. Rev. Lett.* **2000**, *85* (25), 5436−5439.

NL061531+